The Co_2Al_9 Structure Type Revisited

Magnus Boström*, Helge Rosner, Yurii Prots, Ulrich Burkhardt, and Yuri Grin

Dresden, Max-Planck-Institut für Chemische Physik fester Stoffe

Received September 6th, 2004.

Dedicated to Professor Arndt Simon on the Occasion of his 65th Birthday

Abstract. The centrosymmetric structure of Co_2Al_9 (space group $P2_1/c$, Pearson symbol $mP22$), the isotypic structures of Rh_2Al_9 and Ir_2Al_9 and the slightly distorted acentric structures of Rh_2Ga_9 and Ir_2Ga_9 (space group Pc) were reinvestigated from single crystal X-ray diffraction data. The structure of Rh_2Ga_9 represents a new structure type. The difference between the aluminides and the gallides originates in the details of atomic interactions investigated by the electron localization function and band structure calculations.

Keywords: Intermetallic compounds; crystal structure; chemical bonding

Der Strukturtyp Co_2Al_9 erneut untersucht

Inhaltsübersicht. Die zentrosymmetrische Struktur der Verbindung Co_2Al_9 (Raumgruppe $P2_1/c$, Pearson-Symbol $mP22$), die isotypen Strukturen Rh_2Al_9 und Ir_2Al_9, sowie die leicht verzerrten azentrischen Strukturen Rh_2Ga_9 und Ir_2Ga_9 (Raumgruppe Pc) wurden auf der Basis der Einkristall-Röntgenbeugungsdaten erneut untersucht. Rh_2Ga_9 stellt einen neuen Strukturtyp dar. Der Unterschied zwischen den Aluminiden und den Galliden wird durch interatomare Wechselwirkungen verursacht, die mit Hilfe der Elektronen-Lokalisierung-Funktion und Bandstruktur-Berechnungen untersucht wurden.

1 Introduction

Four representatives of the Co_2Al_9 structure type [1] have been found exclusively among aluminides and gallides of the cobalt group transition metals: Rh_2Al_9, Ir_2Al_9 [2], Rh_2Ga_9 and Ir_2Ga_9 [3]. Except for Co_2Al_9, none of the structures have previously been refined from single crystal or powder diffraction data. During an ongoing study of the binary compounds in the Ir−Ga system, it was found that Ir_2Ga_9 is not correctly described as isotypic to Co_2Al_9. This prompted a detailed crystal structure re-investigation of all the five known compounds previously assigned to the Co_2Al_9 structure type.

2 Experimental

Single crystals of the aluminides T_2Al_9 (T = Co, Rh, Ir) were prepared starting from mixtures of the elements with nominal compositions (Table 1) corresponding to the equilibrium region between the relevant phase and its melt [4]. The mixtures were weld-sealed in tantalum containers fitted with tantalum filters, which were manufactured from tantalum plate with five holes of 0.5 mm diameter. These containers were subsequently sealed inside evacuated quartz tubes. Heat treatment conditions are listed in Table 1. The melt was removed by high temperature centrifugation-aided filtration (HT-CAF, [5]) at elevated temperature immediately after the heat treatment. The solid phase remaining after the separation was found to be single crystals of the respective T_2Al_9 phase. Preparation of the gallides T_2Ga_9 (T = Rh, Ir) was performed analogously, but in quartz ampoules with quartz wool filters instead of tantalum containers.

Table 1 Preparation of the T_2Al_9 and T_2Ga_9 compounds (T = Co, Rh, Ir). Educts: Co, Chempur, 99.5 %; Rh, Chempur, 99.9 %; Ir, Lamprecht, 99.9 %; Al, Chempur, 99.99 %; Ga, Chempur, 99.999 %.

Compound	Starting composition	Heat treatment
Co_2Al_9	0.208 g Co; 0.826 g Al ($Co_{0.103}Al_{0.897}$)	8 days at 800 °C
Rh_2Al_9	0.158 g Rh; 0.378 g Al ($Rh_{0.099}Al_{0.901}$)	8 days at 800 °C
Ir_2Al_9	0.232 g Ir; 0.299 g Al ($Ir_{0.098}Al_{0.902}$)	7 days at 800 °C
Rh_2Ga_9	0.058 g Rh; 0.938 g Ga ($Rh_{0.040}Ga_{0.960}$)	5 days at 500 °C
Ir_2Ga_9	0.079 g Ir; 0.921 g Ga ($Ir_{0.030}Ga_{0.970}$)	12 h at 500 °C + cooling down to 100 °C by 2 °C/h

Metallographic analysis on Ir_2Ga_9 was performed on resin mounted samples polished by the use of 1 μm polycrystalline diamond powder followed by 0.25 μm alumina finishing. Bright-field contrast as well as polarization contrast procedures in an optical microscope were used to investigate the homogeneity of the microstructure as well as grain or domain orientations. Image filters were applied to the CCD images of the microstructures for contrast enhancement.

* Dr. Magnus Boström
c/o Prof. Dr. Yuri Grin
Max-Planck-Institut für Chemische Physik fester Stoffe
Nöthnitzer Str. 40
D-01187 Dresden
FAX: 0351-4646-4002
e-mail: bostroem@cpfs.mpg.de
grin@cpfs.mpg.de

  DOI: 10.1002/zaac.200400418

Table 2 Data collection and handling

Crystal data					
Composition	Co_2Al_9	Rh_2Al_9	Ir_2Al_9	Rh_2Ga_9	Ir_2Ga_9
Crystal system			monoclinic		
Space group	$P2_1/c$	$P2_1/c$	$P2_1/c$	Pc	Pc
Z	2	2	2	2	2
a (Å)*	6.2163(3)	6.3501(3)	6.3779(3)	6.4164(4)	6.4329(2)
b (Å)*	6.2883(3)	6.4266(2)	6.4318(2)	6.4119(5)	6.4099(2)
c (Å)*	8.5587(3)	8.7181(3)	8.7337(3)	8.7847(5)	8.8068(4)
β (°)*	94.772(4)	94.809(3)	94.776(4)	93.390(5)	93.464(4)
V (Å^3)*	333.4	354.5	357.0	360.8	362.5
Density calc. (g cm^{-3})	3.5916(8)	4.2016(4)	5.8350(6)	7.668(1)	9.2688(9)
Crystal form			Irregular		
Crystal size (mm^3)	0.030× 0.045× 0.055	0.040× 0.030× 0.025	0.025× 0.030× 0.040	0.040× 0.025× 0.015	0.045× 0.050× 0.025
Colour			Grey, metallic lustre		
Absorption coefficient (mm^{-1})	6.05	5.66	38.25	37.35	69.30
Data collection					
Diffraction system			Rigaku AFC7 Mercury CCD		
Radiation, λ (Å)			Mo Kα, 0.71069		
No. of measured reflections	3697	3908	4015	3704	3074
Range of $h\ k\ l$	$-7 \le h \le 9$ $-7 \le k \le 9$ $-13 \le l \le 13$	$-9 \le h \le 6$ $-9 \le k \le 6$ $-12 \le l \le 12$	$-9 \le h \le 9$ $-7 \le k \le 9$ $-9 \le l \le 13$	$-9 \le h \le 7$ $-9 \le k \le 9$ $-12 \le l \le 10$	$-8 \le h \le 7$ $-8 \le k \le 8$ $-12 \le l \le 8$
Absorption correction			Numerical from crystal shape		
T_{max} / T_{min}	1.13	1.25	1.44	1.40	2.59
R_{int}	0.022	0.024	0.029	0.043	0.031
Refinement					
Refinement on			F		
No. of independent reflections	1129	1013	1228	1547	1663
No. of independent observed reflections	1045	937	1129	1417	1370
Observation criteria			$I > 3\sigma(I)$		
No. of reflections used in refinement	1129	1013	1228	1547	1663
No. of refined parameters	53	53	53	99	99
Weighting scheme			Unit		
$R_{all}(F)$	0.029	0.021	0.019	0.025	0.035
wR_{all} (F)	0.028	0.022	0.022	0.026	0.038
R_{gt} (F)	0.026	0.019	0.017	0.022	0.026
GOF_{all}	1.38	0.92	1.17	0.81	1.68
$\Delta\rho_{max}$, $\Delta\rho_{min}$, (e Å^{-3})	0.73, −0.58	0.92, −0.66	1.65, −2.15	1.49, −1.24	2.55, −1.92
Extinction model			Gaussian isotropic [23]		
Extinction coefficient	0.064(3)	0.043(2)	0.022(1)	0.0145(8)	0.034(2)

* Refined from Guinier powder diffraction data with internal standard.

X-ray powder diffraction patterns of the powdered single crystals were collected with a Huber Imaging Plate Guinier Camera G670 using Cu$K\alpha_1$ radiation (λ = 1.54060 Å) for all samples except that containing Co_2Al_9, for which Co$K\alpha_1$ (λ = 1.78897 Å) radiation was used. Silicon powder (a = 5.43119(1) Å) was added as internal standard for all samples except that of Co_2Al_9, for which LaB_6 (a = 4.15692(1) Å) was used. The lattice parameters were refined from the powder data using the CELREF program [6].

Suitable single crystals for the X-ray diffraction experiment were cleaved with a scalpel under ethanol from the larger ones and then mounted on a thin glass capillary using two component epoxy glue. The data were collected on a Rigaku AFC7 diffraction system equipped with a Mercury CCD detector using Mo$K\alpha$ radiation. Numerical absorption corrections were performed using the CrystalClear program package [7]. The crystal structures were refined with the JANA2000 program [8]. The refined parameters were, for each structure, the scale factor, atomic coordinates, anisotropic displacement parameters and extinction coefficient. The volume fraction of the inversion twins was refined to determine the absolute structure of the gallides. See Table 2 for details about the data collection and handling.

The TB-LMTO-ASA program package [9] with exchange correlation potential according to *Barth* and *Hedin* [10] was used for quantum chemical calculations (LDA). The radial scalar-relativistic Dirac equation was solved to get the partial waves. The calculation within the atomic sphere approximation (ASA) includes corrections for the neglect of interstitial regions and partial waves of higher order [11], hence an addition of empty spheres in the cases of Rh_2Ga_9 and Rh_2Al_9 was not necessary. The following radii of atomic spheres were applied for the calculations on Rh_2Ga_9: r(Rh) = 1.537, 1.542 Å; r(Ga) = 1.574, 1.572, 1.682, 1.661, 1.534, 1.577, 1.596, 1.404, 1.472 Å; on Rh_2Al_9: r(Rh) = 1.524 Å; r(Al) = 1.558, 1.639, 1.568, 1.586, 1.470 Å (see Table 3 for labelling of the atoms). Basis sets containing Rh(5*s*,5*p*,4*d*), Al(3*s*,3*p*) or Ga(4*s*,4*p*) orbitals were employed for the self-consistent calculations with the Rh(4*f*), Ga(4*d*) and Al(3*d*) functions being downfolded.

The electron localization function (ELF) was evaluated according to [12] with an ELF module already implemented within the TB-LMTO-ASA program package [9]. To gain a deeper insight into the chemical bonding, the topology of ELF was analysed with the program Basin [13]. The electron density was integrated in basins, which were bounded by zero-flux surfaces in the ELF gradient.

Table 3 Atomic coordinates and displacement parameters (in Å^2) for the compounds with the Co_2Al_9 and Rh_2Ga_9 structure types (T – transition metal)

		Co_2Al_9	Rh_2Al_9	Ir_2Al_9	Rh_2Ga_9	Ir_2Ga_9
T1a	x*	0.73683(5)	0.73661(4)	0.73673(3)	0.7401	0.7393
	y	0.11844(5)	0.12193(4)	0.12194(3)	0.8783(2)	0.8752(1)
	z*	0.16693(4)	0.16845(3)	0.16833(2)	0.1685	0.1683
	U_{eq}**	0.00630(9)	0.00537(7)	0.00409(6)	0.0062(2)	0.0059(3)
T1b	x	–	–	–	−0.7398(2)	−0.7400(1)
	y				0.6239(2)	0.6224(1)
	z				−0.16903(9)	−0.16833(9)
	U_{eq}				0.0066(2)	0.0051(3)
Ga1a / Al1a	x	0.5940(2)	0.5982(2)	0.5988(2)	0.5986(3)	0.5997(6)
	y	0.4664(2)	0.4766(2)	0.4781(3)	0.2369(2)	0.2379(5)
	z	0.23200(9)	0.2304(2)	0.2299(2)	0.2307(2)	0.2264(5)
	U_{eq}	0.0103(2)	0.0100(2)	0.0087(4)	0.0125(4)	0.0109(9)
Ga1b	x	–	–	–	−0.5993(3)	−0.6004(6)
	y				0.2623(2)	0.2635(5)
	z				−0.2260(2)	−0.2325(5)
	U_{eq}				0.0127(4)	0.0111(9)
Ga2a / Al2a	x	0.6101(2)	0.6113(2)	0.6113(2)	0.5997(3)	0.6130(6)
	y	0.6913(2)	0.6946(2)	0.6931(3)	0.4453(2)	0.4456(5)
	z	0.50228(9)	0.5024(2)	0.5007(2)	0.5084(2)	0.4999(5)
	U_{eq}	0.0095(2)	0.0093(2)	0.0081(4)	0.0139(4)	0.0113(9)
Ga2b	x	–	–	–	−0.6141(3)	−0.6018(6)
	y				0.0557(2)	0.0545(5)
	z				−0.5023(2)	−0.5076(5)
	U_{eq}				0.0123(4)	0.0127(9)
Ga3a / Al3a	x	0.9123(2)	0.9048(2)	0.9033(2)	0.9109(3)	0.8929(6)
	y	0.7897(2)	0.7869(2)	0.7850(3)	0.5491(2)	0.5285(5)
	z	0.27056(9)	0.2722(2)	0.2721(2)	0.2678(2)	0.2791(5)
	U_{eq}	0.0106(2)	0.0104(2)	0.0093(4)	0.0162(4)	0.0121(8)
Ga3b	x	–	–	–	−0.8958(3)	−0.9091(6)
	y				0.9691(2)	0.9566(5)
	z				−0.2828(2)	−0.2687(5)
	U_{eq}				0.0137(4)	0.0145(9)
Ga4a / Al4a	x	0.7837(2)	0.7869(2)	0.7859(2)	0.7816(3)	0.7979(6)
	y	0.1143(2)	0.1077(2)	0.1055(3)	0.8461(3)	0.8616(5)
	z	0.45675(9)	0.4604(2)	0.4609(2)	0.4614(2)	0.4568(5)
	U_{eq}	0.0096(2)	0.0098(2)	0.0086(4)	0.0165(4)	0.014(1)
Ga4b	x	–	–	–	−0.7998(3)	−0.7842(6)
	y				0.6343(2)	0.6573(6)
	z				−0.4570(2)	−0.4622(5)
	U_{eq}				0.0156(4)	0.016(1)
Ga5 / Al5	x	0	0	0	−0.0320(3)	0.0299(6)
	y	0	0	0	0.7611(3)	0.7415(6)
	z	0	0	0	−0.0302(2)	0.0272(5)
	U_{eq}	0.0119(3)	0.0157(4)	0.0162(7)	0.0296(6)	0.027(1)

* Fixed during refinement of the gallides.

** $U_{eq} = \frac{1}{3}\sum_i \sum_j U_{ij} a_i^* a_j^* a_i a_j$

This method is analogous to the procedure proposed by *Bader* for electron density analysis [14] and provides electron counts for each basin. The electron counts reveal basic information for the description of the bonding situation [15, 16].

A full-potential non-orthogonal local-orbital calculation scheme (FPLO, [17]) was applied, within the L(S)DA, in order to obtain more accurate values of the total energy for different symmetry (space groups Pc and $P2_1/c$) and detailed electronic structure information (e.g. electronic DOS). No optimisation of the atomic parameters was performed and the experimentally determined values were used for all calculations. In the scalar-relativistic calculations, the exchange and correlation potential of *Pedrew* and *Wang* [18] was used. The basis sets of Rh(4*s*,4*p*,5*s*,5*p*,4*d*), Ir(5*s*,5*p*,6*s*,6*p*,5*d*), Al(2*s*,2*p*,3*s*,3*p*,3*d*) and Ga(3*s*,3*p*,4*s*,4*p*,4*d*) states were employed and the lower lying sets were treated fully relativistically as core states. The inclusion of the Rh (4*s*,4*p*), Ir (5*s*,5*p*), Ga (3*s*,3*p*) and Al (2*s*,2*p*) states into the valence range was necessary to account for the non-negligible overlap of these states. The spatial extension of the basic orbitals, controlled by a confining potential $(r/r_0)^4$, was optimised to minimise the total energy [19]. A k-mesh of 396 points in the irreducible part of the Brillouin zone was used to ensure accurate density of states information. To be able to compare the total energy values for different structures, the calculations were performed in the space group Pc. To account for the symmetry of the space group $P2_1/c$, the additional elements of symmetry were introduced by the use of the atomic coordinates strictly obeying these symmetry elements. Both possible absolute structures in the space group Pc were calculated to prove the quality of the numerical calculations, resulting in identical values of the total energy ($\Delta E_{tot} < 10^{-8}$ Hartree).

3 Results and discussion

Metallographic investigations of the single crystals of Ir_2Ga_9 did not reveal any signs of macroscopic twinning. None of the crystals showed any signs of containing more than one grain (Fig. 1).

We note that the monoclinic angle of the unit cells of Rh_2Ga_9 and Ir_2Ga_9 refined in the present study (see Table

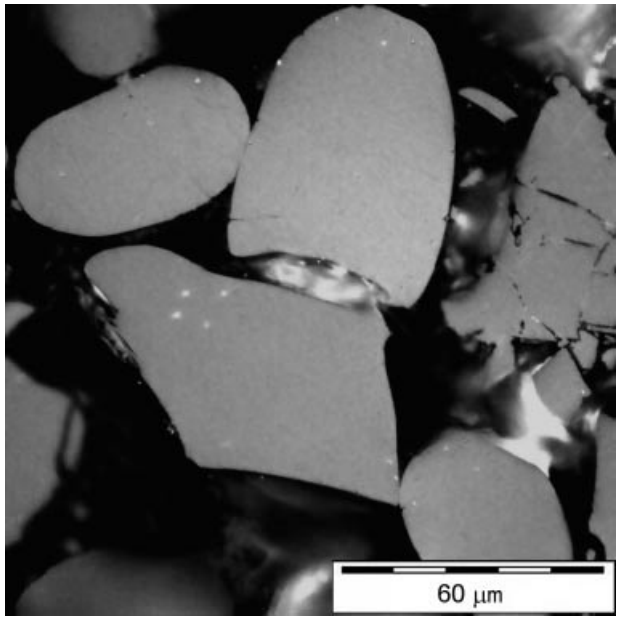

Fig. 1 Homogeneous microstructure of Ir_2Ga_9 crystals (grey) mounted in phenolic resin (dark) [objective 20×, polarized light, contrast-enhanced CCD image].

2) differs more than 3° from those in [3]. The other cell parameters differ less than 0.05 Å.

The crystal structures of Rh_2Ga_9 and Ir_2Ga_9 were first refined in the space group $P2_1/c$, using the published atomic parameters of Co_2Al_9 as starting model. Most of the Ga atoms showed stronger anisotropy in atomic displacement in comparison with the corresponding Al atom in T_2Al_9. Especially pronounced anisotropic displacement was observed for Ga5, positioned at the inversion center (Fig. 2). Additionally, a detailed analysis of the single crystal diffraction data revealed that the 050 and $0\bar{5}0$ reflections, which should be systematically absent in the space group $P2_1/c$ due to the two-fold screw axis, were clearly observed in the recorded diffraction patterns of both gallides (I / $\sigma(I)$ = 18.5 for Rh_2Ga_9 and I / $\sigma(I)$ = 5.7 for Ir_2Ga_9). The difference is hard to recognise in powder diffraction data, as the reflections in question are overlapped by other strong reflections. The observation of these reflections that should be systematically extinct in the space group $P2_1/c$ leads to another extinction class with the two possible space groups $P2/c$ and Pc. For structural reasons, the centrosymmetric space group $P2/c$ is irrelevant, since this space group is not appropriate for the description of the packing of the polar polyhedra in the Co_2Al_9 structure type. Thus the space group Pc was choosen, whereby all residual values decreased significantly ($R_{gt}(F)$ from 0.062 to 0.021 for Rh_2Ga_9 and from 0.037 to 0.024 for Ir_2Ga_9). The x and z coordinates for Ir1a and Rh1a were fixed to the coordinates of the corresponding atom obtained in the refinement in the space group $P2_1/c$ in order to define the origin. The y coordinates in the T_2Ga_9 structures differ from those in T_2Al_9 by 0.25, due to the different location of the glide mirror plane perpendicular to [010] in the space groups $P2_1/c$ and Pc.

The volume fraction of the inversion twin was refined in order to obtain the absolute structure, a method that can be used as analogous to the Flack parameter [20]. In the case of Rh_2Ga_9, the volume fraction of the inversion twin was found to be 0.03(3), which indicated that the absolute structure of the investigated crystal of Rh_2Ga_9 was correctly described. In the case of Ir_2Ga_9, the fraction of the inversion twin was refined to be 0.57(4), but without a decisive decrease in residuals (from $R_{gt}(F)$ = 0.026 to $R_{gt}(F)$ = 0.024). Additionally, the difference in residuals between the possible absolute structures was extremely small (0.003 in $R_{gt}(F)$). Together with the results of optical metallography, this suggest that the Ir_2Ga_9 crystal is not twinned. Establishing of the absolute structure is in this case not trivial, due to the nearly double as strong relative contribution of Ir compared with Rh to the diffraction intensities in combination with the practically centrosymmetric transition metal positions in Ir_2Ga_9 compared with Rh_2Ga_9. The second possibility that was considered is that the crystals of Ir_2Ga_9 are roughly racematically twinned at a scale not observable with a light-optical microscope. However, the fact that the chemically very similar compound Rh_2Ga_9 did not show any sign of twinning from the diffraction data, strongly suggests the absence of twinning also in Ir_2Ga_9.

Refinement of the crystal structures of Rh_2Ga_9 and Ir_2Ga_9 in the space group Pc markedly reduced the aniso-

Table 4 Interatomic distances (in Å) for T_2Al_9 and T_2Ga_9 compounds (T = Co, Rh, Ir).

Distances	Co_2Al_9	Rh_2Al_9	Ir_2Al_9	Rh_2Ga_9 in Pc	Ir_2Ga_9 in Pc	Rh_2Ga_9 in $P2_1/c$	Ir_2Ga_9 in $P2_1/c$
T − (Al, Ga)[a]	2.443 − 2.538	2.517 − 2.601	2.527 − 2.601	2.507 − 2.690	2.537 − 2.672	2.545 − 2.633	2.549 − 2.655
T − (Al5, Ga5)	2.379	2.445	2.451	2.457 − 2.463	2.459 −2.461	2.437	2.441
$1 - \frac{T - (Al5, Ga5)}{T - (Al, Ga)} \times 100\,\%$[b]	2.6	2.9	3.0	1.8 − 2.0	3.1 − 3.2	4.2	4.2
Al − Al, Ga − Ga[c]	2.706 − 2.941	2.750 − 2.993	2.735 − 2.964	2.699 − 2.971	2.671 − 2.987	2.712 − 2.992	2.719 − 2.954
Al5 − Al, Ga5 − Ga[d]	2.701 − 2.783	2.740 − 2.868	2.738 − 2.888	2.681 −2.990	2.654 − 2.996	2.755 −2.875	2.750 − 2.895

[a] All T − (Al, Ga) distances except T−(Al5, Ga5)
[b] Relative difference between the shortest heteroatomic distance (T−(Al5, Ga5)) and the next shortest heteroatomic distance in the structure.
[c] All Al−Al or Ga−Ga distances except those including Al5 or Ga5.
[d] Homoatomic distances involving Al5 or Ga5.

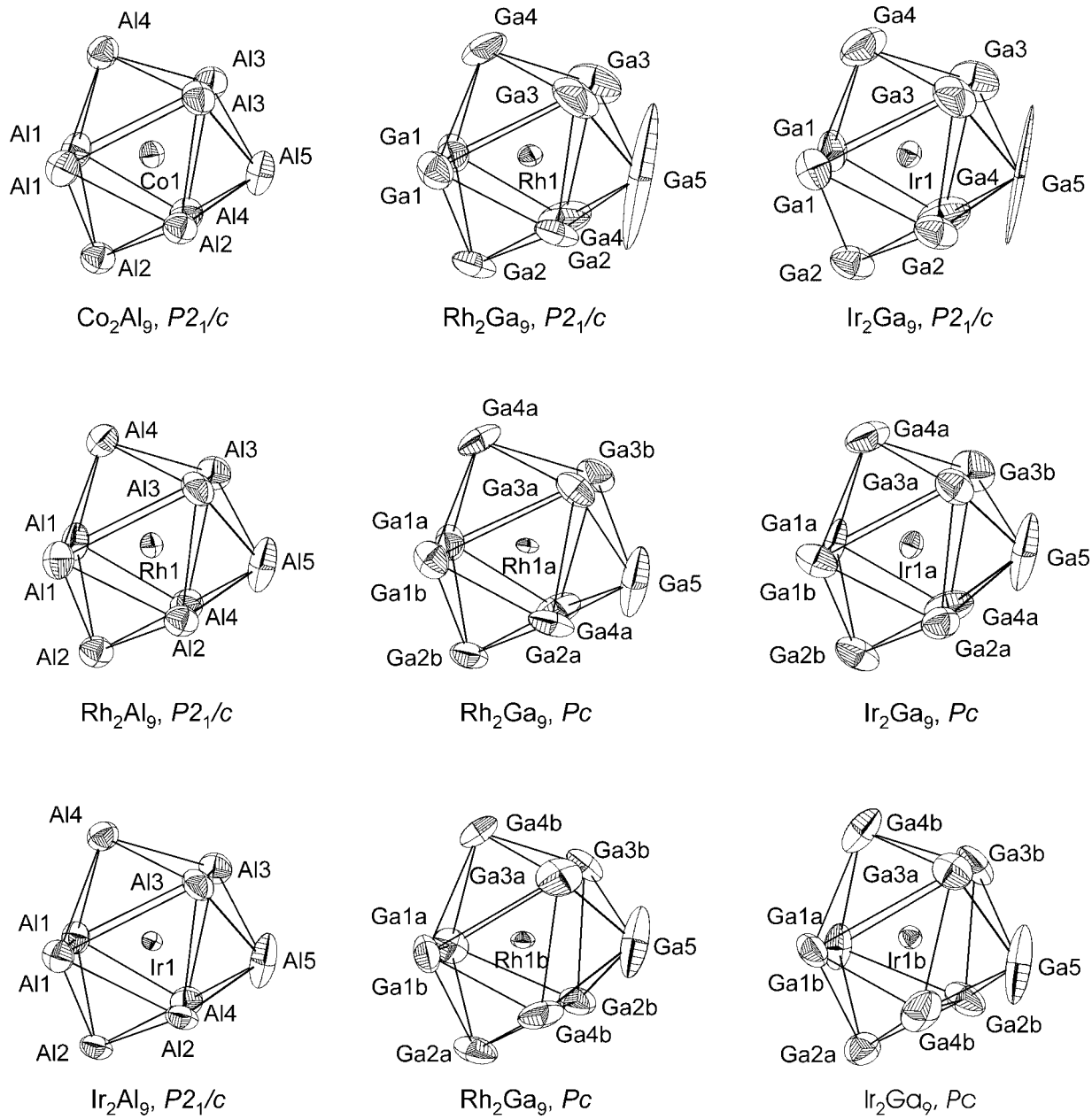

Fig. 2 Coordination polyhedra around the transition metals with atomic displacement ellipsoids (99.5 % probability) in the crystal structures of T_2Al_9 and T_2Ga_9 (T = Co, Rh, Ir). For the gallides, models obtained both in the space group $P2_1/c$ and in the space group Pc are shown.

tropy of the displacement of the Ga atoms in comparison with the refinement in space group $P2_1/c$ (Fig. 2). The displacement ellipsoids approached the size of those of Al in the aluminides T_2Al_9. Final values of atomic coordinates and displacement parameters for the gallides T_2Ga_9 are presented in Table 3. Since the determination of the absolute structure of Ir_2Ga_9 failed, Table 3 contains the crystallographic parameters for the absolute structure analogous to Rh_2Ga_9 for facilitating comparison.

None of the aluminides showed any sign of deviation from the symmetry of the space group $P2_1/c$, and the 050 and $0\bar{5}0$ reflections were absent in the single crystal diffraction data sets. Final atomic coordinates and displacement parameters for the aluminides are shown in Table 3. Relevant interatomic distances are listed in Table 4.

The Co_2Al_9 structure type can be described in terms of single-capped square antiprismatic coordination polyhedra around the transition metal atoms (Fig. 3, top). These polyhedra build up zig-zag strands parallel to the c axis. The strands are arranged in a simple quadratic rod packing (see Fig. 3, bottom). It should be noted that a single-capped square antiprism can also be described as a trigonal prism with capped rectangular faces, a view used in Fig. 2. However, the single capped square antiprism lends itself better for the use in the structural description in Fig. 3. Another advantage is that it better reflects the relation of the Co_2Al_9

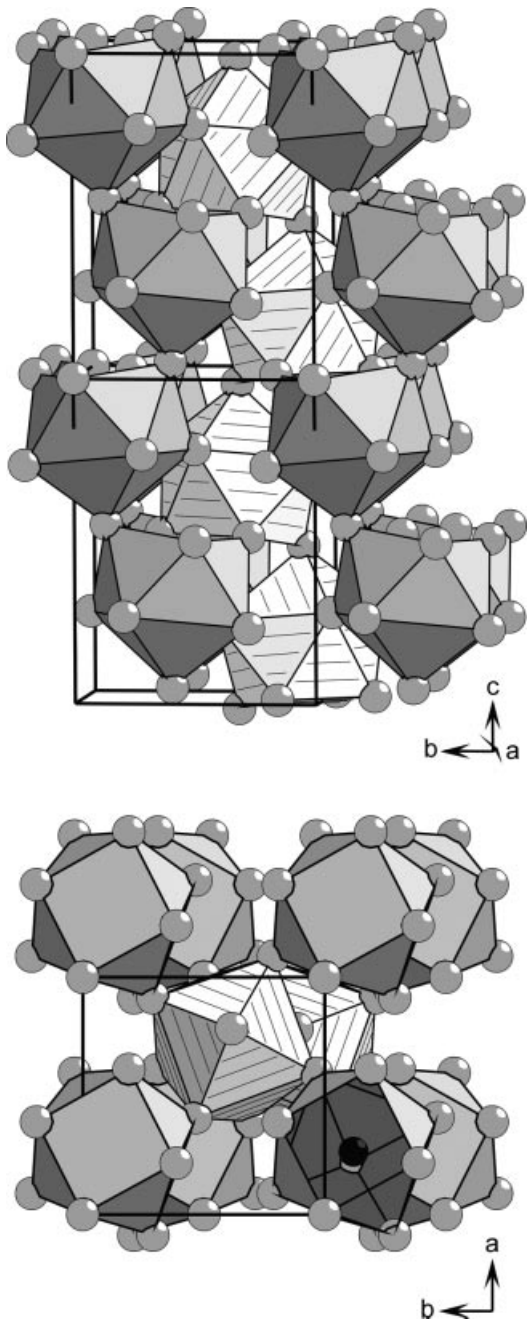

Fig. 3 Views along [100] (top) and [001] (bottom) of the Co_2Al_9 structure. Monocapped square antiprisms [$CoAl_9$] with different orientations relative to [001] are drawn light grey hatched and grey, respectively. The antiprism down to the right is drawn with one face open, exposing the centering Ir atom.

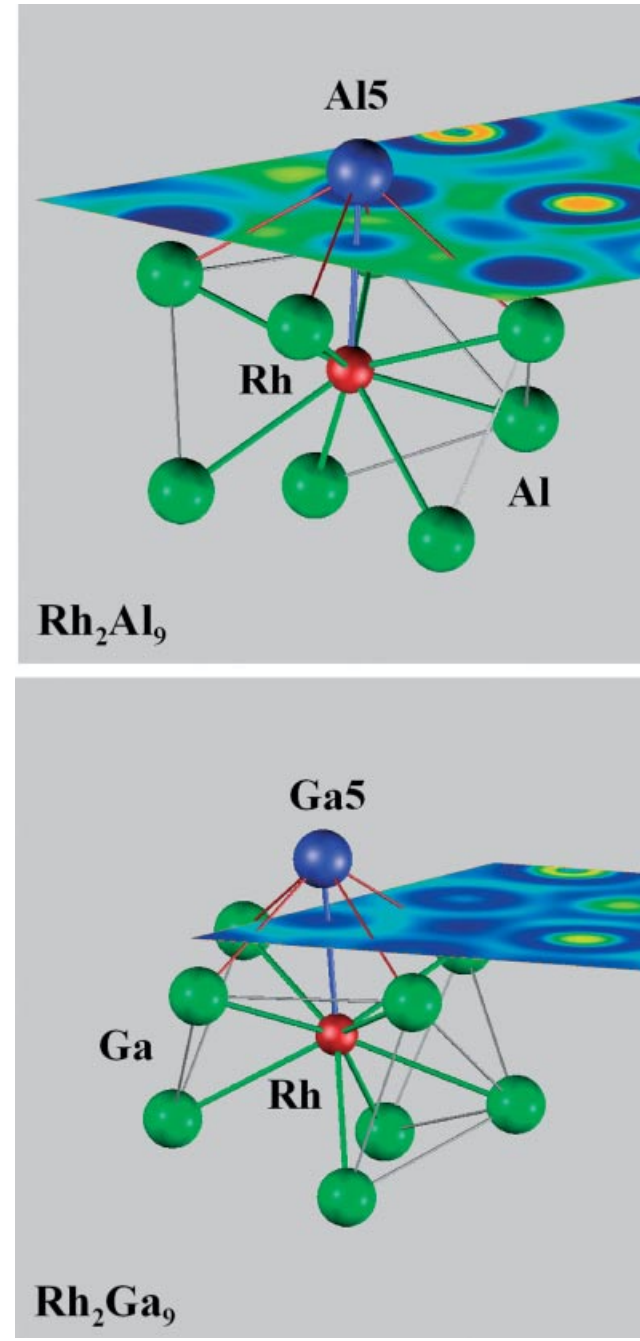

Fig. 4 Electron localization function for Rh_2Al_9 (top) and Rh_2Ga_9 (bottom) in the vicinity of the Rh−Al5 and Rh−Ga5 bonds (blue sticks). In the two-dimensional sections of ELF nearly normal to the T−(Al5,Ga5) bonds, the high values of ELF are represented by bright orange for Rh_2Al_9 and greenish blue for Rh_2Ga_9.

and Rh_2Ga_9 structures to the parent structure of $CuAl_2$, where the tetragonal symmetry of the polyhedron is clearly exhibited.

The structure of Rh_2Ga_9 represents a new structure type due to the different space group caused by the slight distortion of the Co_2Al_9 archetype structure. In the low-symmetry gallides, each of the zig-zag strands contains polyhedra of only one of the two crystallographically independent transition metal atoms. The atom Ga5, which is located at the inversion center in the Co_2Al_9 archetype, is the strongest contributor to the observed symmetry breaking in the gallides, with a shift of 0.32 Å along the [101] direction in Ir_2Ga_9. All other atoms shift less than 0.12 Å with average displacement of 0.06 Å.

The T−(Al5,Ga5) distances are in all the structures 1.8 − 3.2 % shorter than the rest of the T−(Al, Ga) distances

within the structures (Table 4). When the gallides were refined with the symmetry constraints of the space group $P2_1/c$, i.e. Ga5 is placed at an inversion center, the resulting difference was 4.2 % in both gallide structures. The symmetry reduction evidently offers a route to relieve the geometric strain in the gallides. The geometric strain that exists mainly around Al5 in the aluminides does not seem to be enough to cause a reduction of the symmetry. However, one may note that the atomic displacement of Al5 in the aluminides are the largest among all atoms in those structures. The unit cell volumes for the aluminides T_2Al_9 and the gallides T_2Ga_9 differ only by 1−2 %. Hence, the size effect may not be enough to cause the symmetry reduction. We suggest that the origin of this effect has to be found in the special features of the bonding interactions.

The electron localization function reveals that two-center covalent Al−Al and Ga−Ga interactions, especially between the antiprisms, play a key role in the stabilisation of the different structures of Rh_2Al_9 and Rh_2Ga_9. This is in good agreement with the results of the bonding analysis in $PdGa_5$ [21] and $CuAl_2$ [22] where the covalent interactions were found primarly between Ga (Al) atoms belonging to neighbouring tetragonal antiprisms. The difference between the two structures can be observed within the vicinity of the Rh−Al5 and Rh−Ga5 bonds inside the antiprisms (Fig. 4). For Rh_2Al_9, the ELF attractors are located at the Al5−Al bonds (red in Fig. 4). In Rh_2Ga_9 the attractors are shifted from the Ga5−Ga bonds toward the Rh−Ga5 contact, forming a ring attractor set similar to the Sc−Ga bonds observed in [16] for ScGa molecule. This suggests a more directional Rh−Ga5 interaction in comparison with Rh−Al5, which inhibits the achievement of higher symmetry in the the two gallides T_2Ga_9.

This behaviour is also confirmed by the band structure calculations for Ir_2Al_9 and Ir_2Ga_9. The electronic density of states (DOS) of Ir_2Al_9 (Fig. 5, top) shows a similar picture for both space groups with a relatively low density of states at the Fermi level. The overlap of the Ir-4d and Al-3(s+p) contributions in the valence region suggests bonding interaction between Ir and Al, (cf. ELF analysis). A pronounced difference between the structures with different symmetry is observed only in the middle of this region (-5 eV $\leq E \leq -3$ eV). This leads to the conclusion that the difference between the structure variants crystallising in the space groups Pc and $P2_1/c$ respectively is caused mainly by the difference in the interactions between Ir and Al compared with the interactions between Ir and Ga. This is in good agreement with the ELF analysis. Indeed, for Ir_2Al_9 the variant with the symmetry $P2_1/c$ has a total energy lower by 80 meV in comparison with the Pc variant. This result is in full agreement with the structural data, showing a clear preference for the space group $P2_1/c$ for the aluminides T_2Al_9.

A similar situation is realised in the DOS of Ir_2Ga_9 (Fig. 5, bottom). In this case, besides the Ga−Ga bonds, bonding interactions between Ir and Ga can be derived from the overlap of Ir and Ga contributions in the valence region.

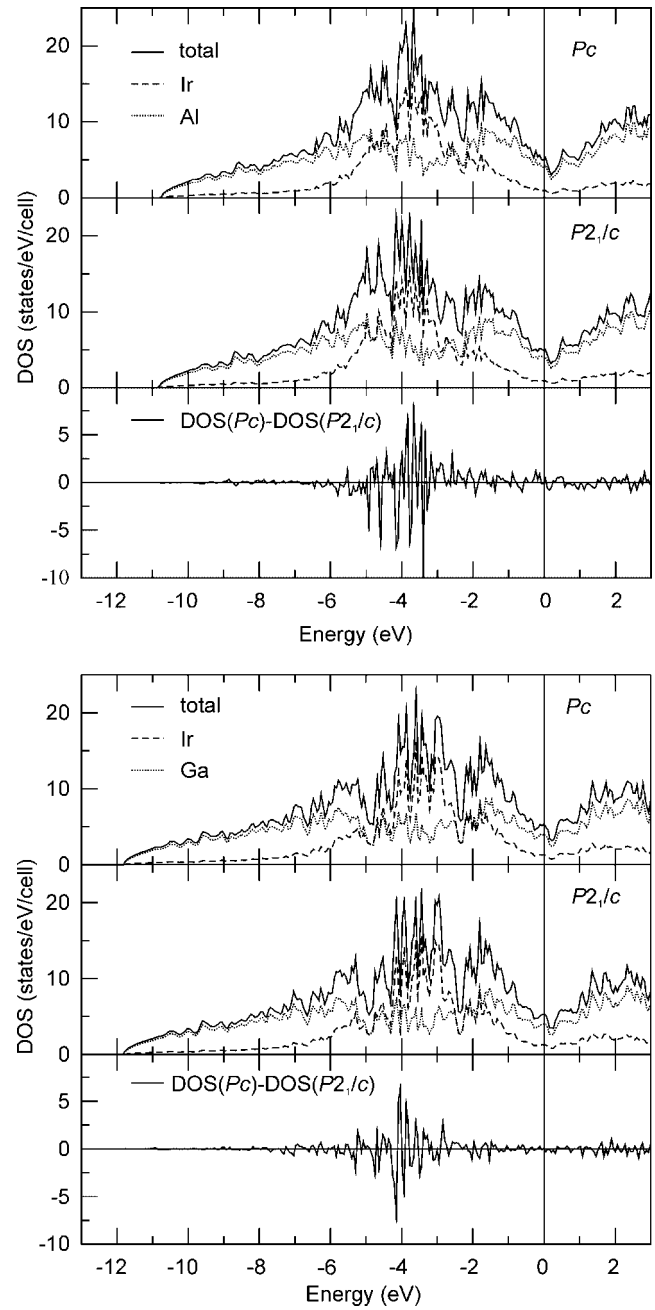

Fig. 5 Electronic density of states (DOS) for Ir_2Al_9 (top) and Ir_2Ga_9 (bottom). For both compounds the total DOS together with the contributions of Ir and Al(Ga) states are shown for both structures with the symmetry of the space groups Pc (DOS(Pc)) and $P2_1/c$ (DOS($P2_1/c$)). The differences between the calculations are presented in form of difference density of states (DOS(Pc) − DOS($P2_1/c$)).

The difference DOS reveals the largest deviation in the same region as in the case of Ir_2Al_9, but the difference is remarkably smaller in comparison with Ir_2Al_9. This fact finds its confirmation in the total energy calculation. Both symmetrically different structural variants differ in energy by only ~1 meV, in favour for the $P2_1/c$ variant due to the very small energy difference. This is not a direct confirmation of the structural data preferring the Pc variant, but

the tendency of structural changes from T_2Al_9 to T_2Ga_9 compounds is illustrated clearly from these calculations.

Further details of the crystal structure investigation can be obtained from Fachinformationszentrum Karlsruhe, 76344 Eggenstein-Leopoldshafen, Germany, (fax. (49) 7247-808-666; e-mail: crysdata@fiz.karlsruhe.de) on quoting the depository number CSD414301 for Co_2Al_9, CSD414304 for Rh_2Al_9, CSD414302 for Ir_2Al_9, CSD414305 for Rh_2Ga_9 and CSD414303 for Ir_2Ga_9.

References

[1] A. M. B. Douglas, *Acta Crystallogr.* **1950**, *3*, 19.
[2] L. E. Edshammar, *Acta Chem. Scand.* **1968**, *22*, 2822.
[3] L. E. Edshammar. *Acta Chem. Scand.* **1970**, *24*, 1457.
[4] *Binary Alloy Phase Diagrams*, 2nd ed., Ed. T.B. Massalski, ASM International, Materials Park, Ohio, 1990.
[5] M. Boström, S. Hovmöller, *J. Alloys Compd.* **2001**, *314*, 154.
[6] J. Laugier, B. Bochu, CELREF, Laboratoire des Materiaux et du Génie Physique de l'Ecole Supérieure de Physique de Grenoble, France, 2003.
[7] Rigaku/MSC Inc, CrystalClear, Area detector processing software, v. 1.3.5. USA, 2002.
[8] V. Petriček, M. Dušek, *Jana2000. The crystallographic computing system*. Institute of Physics, Praha, Czech Republic, 2000.
[9] O. Jepsen, A. Burkhardt, O. K. Andersen, The Program TB-LMTO-ASA. Version 4.7. Max-Planck-Institut für Festkörperforschung, Stuttgart, 1999.
[10] U. Barth, L. Hedin, *J. Phys.* **1972**, *C5*, 1629.
[11] O. K. Andersen, *Phys. Rev.* **1975**, *B12*. 3060.
[12] A. Savin, H. J. Flad, J. Flad, H. Preuss, H. G. von Schnering, *Angew. Chem.* **1992**, *104*, 185; *Angew. Chem. Int. Ed. Engl.* **1992**, *31*, 185.
[13] M. Kohout, Basin. Version 2.4. Max-Planck-Institut für Chemische Physik fester Stoffe, Dresden, 2004.
[14] R. F. W. Bader, *Atoms in molecules: A quantum theory*, Oxford University Press, Oxford, 1999.
[15] M. Kohout, A. Savin, *Int. J. Quantum Chem.* **1996**, *60*, 875.
[16] M. Kohout, F. R. Wagner, Y. Grin, *Theor. Chem. Acc.* **2002**, *108*, 150.
[17] H. Eschrig, *Optimized LCAO method and the electronic structure of extended Systems.* Springer, Berlin, 1989.
[18] J. P. Perdew, Y. Wang, *Phys. Rev.* **1992**, *B45*, 13244.
[19] K. Koepernik, H. Eschrig, *Phys. Rev.* **1999**, *B59*, 1743.
[20] H. Flack, *Acta Crystallogr.* **1983**, *A39*, 876.
[21] Y. Grin, U. Wedig, F. Wagner, H. G. von Schnering, *J. Alloys Compd.* **1997**, *255*, 203.
[22] Y. Grin, F. R. W. Wagner, M. Kohout, M. Armbrüster, A. Leithe-Jasper, U. Schwarz, U. Wedig, H. G. von Schnering, *J. Solid State Chem.* **2004**, Submitted.
[23] P. J. Becker, P. Coppens, *Acta Crystallogr.* **1974**, *A30*, 129.

